

## Performance of landslide debris-resisting baffles

Clarence E Choi<sup>a\*†</sup> and Raymond P H Law<sup>b</sup>

<sup>a</sup>Department of Civil and Environmental Engineering, The Hong Kong University of Science and Technology, Hong Kong, People's Republic of China; <sup>b</sup>Geotechnical Engineering Office, Civil Engineering and Development Department, the HKSAR Government, Hong Kong, People's Republic of China

(Received 22 April 2015; accepted 6 August 2015)

Arrays of landslide debris baffles are commonly installed upstream of rigid barriers in Hong Kong to dissipate flow energy impacting a rigid barrier. Currently, baffles are installed using prescriptive and empirical approaches in Hong Kong without design recommendations. Given the engineering value of baffles, an improved understanding of their interaction mechanisms is warranted. Flume modelling and numerical back analysis using the discrete element method (DEM) were adopted to study the influence of landslide debris baffles on impact on a downstream terminal rigid barrier. Froude scaling was used to dynamically characterise the flow. The optimum geometrical configuration was examined. The results revealed that an array of baffles is effective in reducing the peak dynamic impact induced by debris on a rigid barrier and that overflow processes need to be controlled. Baffle heights exceeding 1.5 times the approach flow depth ( $h$ ) exhibited little incremental influence on reducing the peak dynamic impact forces induced on the rigid barrier. At least two staggered rows are required to effectively intercept discharge from the first row and reduce the frontal debris impact force. The optimum spacing between successive rows ( $L$ ) and transverse blockage is  $L/D = 3$  ( $D$  is the slit opening) and 30%, respectively.

**Keywords:** landslide debris; baffles; impact; physical modelling; discrete element method

### Introduction

Hong Kong has a total area of about 1100 km<sup>2</sup> and 60% of this is comprised of natural terrain. Steep hillsides coupled with seasonal torrential rainfall of up to 2200 mm per year are ideal conditions for slope failure. As development gradually encroaches toward natural hillsides and weather patterns become erratic, the risks associated with landslide debris hazards will undoubtedly increase. It is evident from the natural terrain landslides and debris flows which occurred in North Lantau on 7 June 2008 (Figure 1) that landslide debris hazards are a real threat in Hong Kong. The highway to the airport was blocked by about 400 m<sup>3</sup> of landslide debris for up to 16 hours. Had the landslide occurred in a more densely populated area, the consequence may have been disastrous.

Structural countermeasures such as flexible [2] and rigid [3,4] barriers are most commonly adopted on natural hillsides in Hong Kong. Rigid barriers constructed using reinforced concrete are attractive options since they can resist large dynamic impact loads and bending moments. It is a common practice to install an array of baffles upstream of a rigid barrier in anticipation of reducing the dynamic impact load induced on the rigid barrier. However, the installation of baffles currently relies on prescriptive and empirical approaches in Hong Kong. Design recommendations are not available since

the impact mechanisms are still not well understood. Figure 2 shows an array of rectangular baffles installed in a deposition basin on Lantau Island, Hong Kong.

Baffle research has been well established in hydraulic engineering [6,7] and investigations of avalanche breaking mounds have been carried out (Jóhannesson et al. 2009; [8]). Despite the availability of relevant research in the literature, it is stressed that since the flow behaviour of debris flows is complex and dynamically distinct, recommendations from hydraulic engineering and avalanche research are not entirely applicable to landslide debris problems. Recent research has been carried out on debris flow baffles using flume modelling [9,10] and the discrete element method (DEM) [11–13] to study the interaction and impact mechanisms. Despite the engineering value of these recent studies, they have yet to be amalgamated into coherent preliminary recommendations for potential applications in Hong Kong. This study serves to review the existing relevant research and recommend an optimum configuration for landslide debris baffles.

### Froude scaling

Dynamic similarity is achieved in this study by adopting a hydrodynamic approach and capturing only the most

\*Corresponding author. Email: [cechoi@ust.hk](mailto:cechoi@ust.hk)

†The author was 35 years old or younger at the time of his/her paper submission.



Figure 1. North Lantau Landslide in 2008.[1]



Figure 2. Baffles installed upstream of the rigid barrier on Lantau Island, Hong Kong.[5]

dominant forces. Hübl et al. [14] and Armanini et al. [15] both identified the Froude number ( $Fr$ ) as a key dimensionless parameter for scaling debris flow impact on structures.  $Fr$  is given as follows:

$$Fr = v/\sqrt{gh}, \quad (1)$$

where  $v$  is the flow velocity,  $g$  is the gravitational acceleration and  $h$  is the approach flow depth. Open channel flows are driven by gravitational forces and impact on flow impeding structures is strongly influenced by changes in momentum, hence  $Fr$  is ideal for this study.

Channelised debris flow can be characterised with  $Fr$  ranging from 0 to 8 based on field observations.[14]

#### Flume modelling

A rectangular flume model of 5 m in length was used to study flow interaction with baffles (Figure 3).[9] The channel has a base width of 200 mm and can vary in inclination from  $0^\circ$  to  $50^\circ$ . The storage container is installed in the most upstream end of the flume and has a maximum volume of  $0.03 \text{ m}^3$ . Debris within the storage container is retained using a spring-loaded door that lifts upward upon deactivation of a magnetic lock securing the door

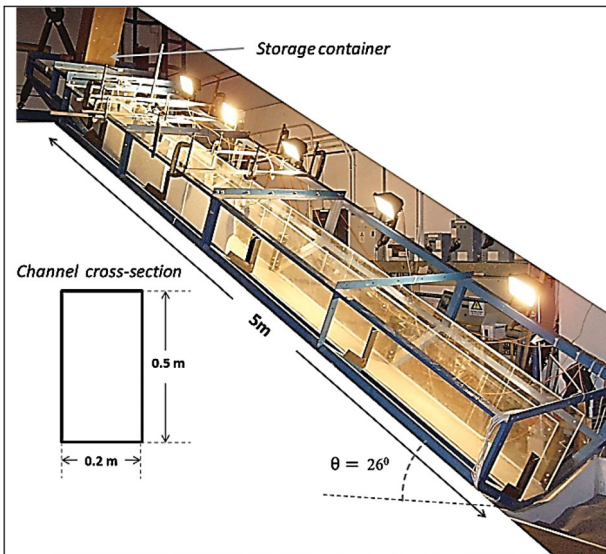


Figure 3. Flume model.[10]

at the base of the channel. The channel walls are constructed using transparent acrylic boards and lined with plastic film.

**Instrumentation**

10 photoconductive sensors (Silonex NORP12 cadmium sulphide) were installed in the base of the channel at intervals of 500 mm. Photoconductive sensors function as light sensors. When debris passes over a sensor, a signal is

generated and sent to the data logger, which captures data at up to 10,000 Hz. Laser displacement sensors (Wenglor YT44MGV80) were reflected off the base of the channel to capture the flow depth profile of debris passing the measurement point. The resolution of these laser sensors is  $\pm 0.2$  mm. High-speed cameras (Prosilica GE640) were mounted to the side and over the baffles to capture the interaction and allow for the dynamics to be interpreted. The high-speed cameras captured images at 200 frames per second with a resolution of  $640 \times 480$  pixels. Reference grids of  $50 \times 50$  mm were imposed on the side channel wall to assist in high-speed imagery interpretation. Lamps (100 W) were installed around the flume to illuminate the channel and enhance the high-speed imagery.

**Model set-up and testing procedures**

Dry uniform Leighton Buzzard Fraction C sand was used for each experiment with particle diameters ranging from 0.3 mm to 0.6 mm. Figure 4 shows a plan view of the model set-up. The appropriate baffle configuration was installed within the channel. A summary of all the test configurations is reported in Ng et al. [16]. The first row of baffles was installed in 800 mm downstream from the storage container to achieve Froude similarity. The container door was secured by activating the magnetic lock at the base of the channel and the springs were then loaded. Debris was placed in the storage container with a target bulk density of  $1680 \text{ kg/m}^3$ . The flume was then

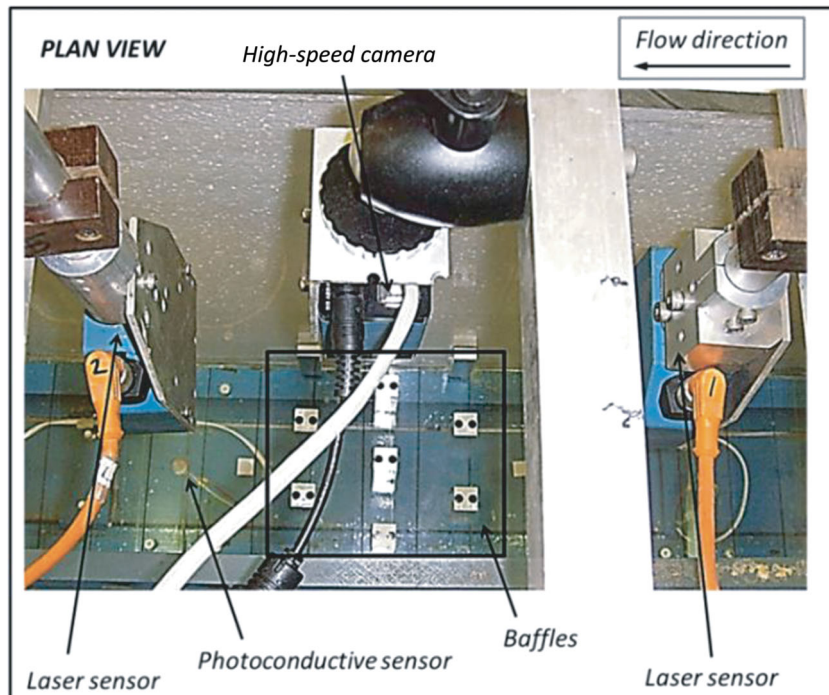


Figure 4. Plan view of model set-up.[10]

hoisted to a channel inclination of  $26^\circ$  using a crane. The instrumentation, high-speed imagery and lighting were prepared. The debris in the storage container was then released by deactivating the magnetic lock and the data logger was activated. A deposition container was positioned at the most downstream end of the flume to capture the debris.

**DEM**

The DEM software package LIGGGHTS [17] was adopted in this study. In the DEM, contact forces and displacements of a stressed assembly of particles are deduced by tracing the movement of individual particles. These particles displace independently from each other and interact at contacts between other particles and boundaries. A linear elastic contact model was adopted.

**DEM model set-up**

Figure 5 shows a side view of the numerical model set-up. The same geometric configuration as the flume experiments was adopted in the DEM model. Planar rigid

walls are used to model the channel base and baffles. For channelised flows, unrealistic particle arrangements can occur at the side walls if a planar rigid wall is used.[18] To eliminate this problem, periodic boundary conditions were introduced to the side walls.[11]

**Modelling procedures and input parameters**

Each numerical analysis is divided into two stages, namely preparation and impact. In the preparation stage, an assembly of discrete elements with random packing is prepared under gravitational acceleration. The debris is located immediately upstream of the first row of baffles. In the impact stage, the discrete elements are given an initial velocity of 2.7 m/s (as measured in the flume experiments) and move downslope to impact the baffle array and terminal rigid barrier. The velocity and the displacement of the discrete elements, as well as the impact force on the rigid barrier, are recorded and analysed throughout the process.

The contact friction angle was set at  $35^\circ$ , which is comparable to the internal friction angle of granular

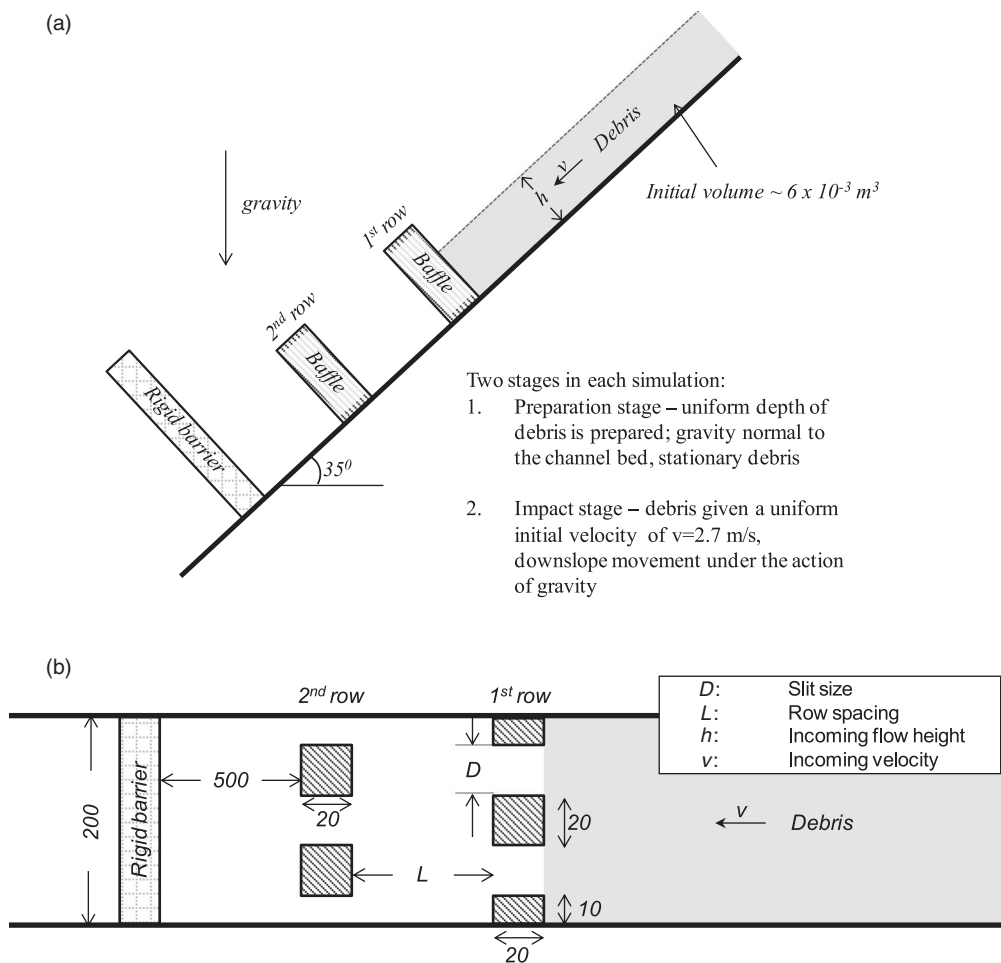


Figure 5. The numerical model set-up: (a) side view; (b) plan view.

Table 1. DEM input parameters.

Input parameter	Value	Comparison with Teufelsbauer et al. [19]
Number of discrete elements	65,000	43,000
Particle diameter (m)	0.005	0.0025
Particle stiffness (N/m)	$1 \times 10^8$	$1 \times 10^8$
Discrete element friction angle	35°	35°
Coefficient of restitution	0.5	N/A

materials adopted in literature.[19–22] Based on the field and laboratory tests conducted by Chau et al. [23], Azzoni and Freitas [24] and Robotham et al. [25], the coefficient of restitution was defined as 0.5. The diameter of the discrete elements was 0.005 m. Due to the constraint of computational capacity, it was not possible to model the motion of the individual grains in debris flow. A summary of the input parameters and a comparison with Teufelsbauer et al. [19] are given in Table 1.

**Calibration**

The observed flow dynamics from the flume experiments were compared with the computed flow dynamics using the DEM. A comparison of flow dynamics serves as a calibration exercise to validate model assumptions and input parameters. Figure 6 shows that the observed and computed flow dynamics using the DEM exhibit reasonable agreement with each other given the constraints of the DEM. Details of the calibration process and selection of input parameters were further discussed in Choi et al. [11].

**Observed interaction mechanisms**

A plan view of a typical flow interaction between granular flow and an array of baffles captured using high-speed imagery is shown in Figure 7. The flow front approaches the first row of baffles (Figure 7(a)) and upon impact, the flow front divides into three granular jets discharging from the slits of the first row (Figure 7(b)). The granular jets impact the second staggered row of baffles and are directed perpendicularly into each other before four thinner granular jets discharge through the slits of the second row (Figure 7(c)). As the interaction progresses, each granular jet thickens (Figure 7(d)) and a ramp-like deposition zone forms upstream of the first row of baffles. Debris is observed overflowing the first row of baffles (Figure 7(e)) and distinct granular vacuums are observed behind each baffle.[26] As debris continues to impact the array of baffles and climb the ramp-like deposition zone, the overflow eventually cascades over the second row of baffles (Figure 7(f)).

**Computed impact mechanisms**

Granular debris impact on a rigid barrier with baffles consists of three key impact mechanisms, namely (i) the granular jet impact stage, (ii) the run-up stage and (iii) the pile-up stage.[13]

The granular jet impact stage on a rigid barrier is characterised by the presence of short peak dynamic impact force, which is related to the generation of a pressure surge due to the rapid deceleration of the granular jet. The run-up stage on a rigid barrier is characterised by the formation of a ramp-like deposition zone which promotes debris climbing up the ramp and impacting the barrier.

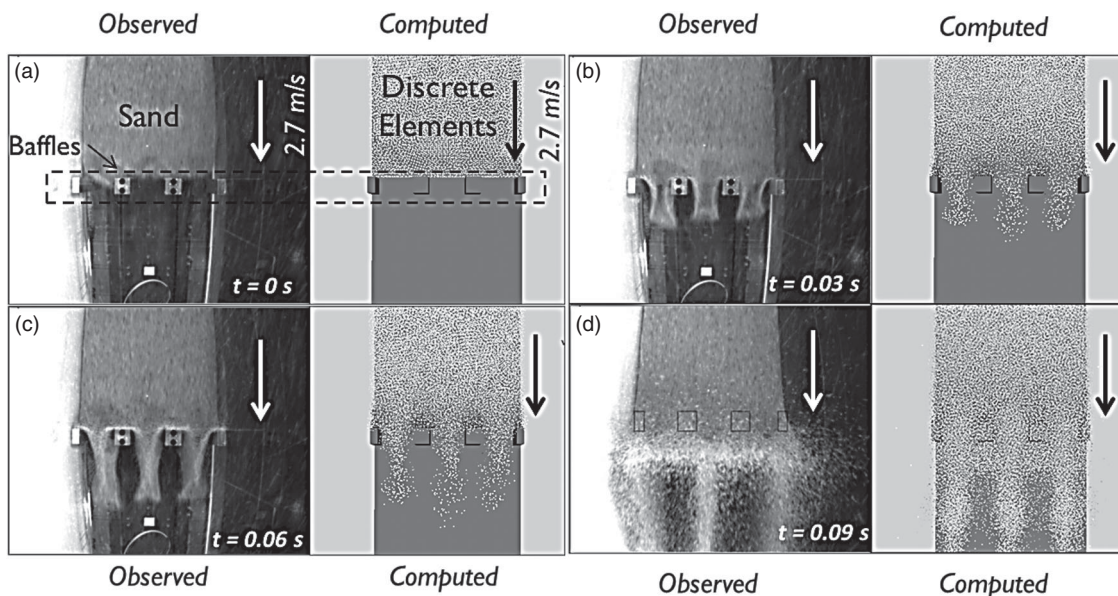


Figure 6. Comparison of the observed and computed flow dynamics.[11]

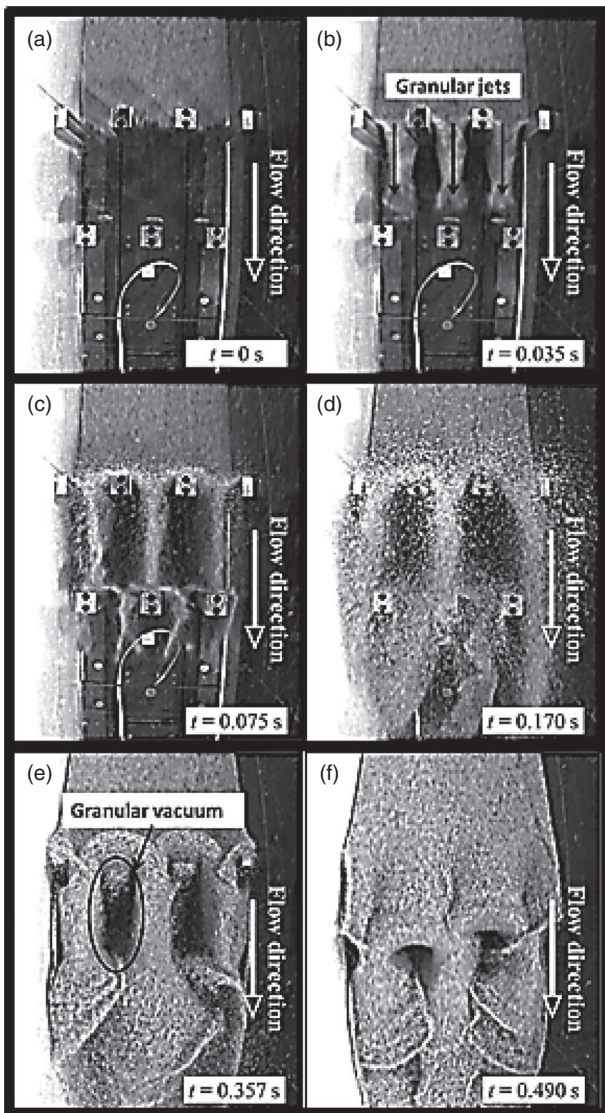


Figure 7. Observed flow dynamics from flume experiments: (a)  $t = 0$  s; (b)  $t = 0.035$  s; (c)  $t = 0.075$  s; (d)  $t = 0.170$  s; (e)  $t = 0.357$  s; (f)  $t = 0.490$  s. [10]

The dynamic impact force is noticeably smaller than the granular jet impact due to the presence of the debris that has already been deposited and accumulated behind the barrier. During the pile-up stage, the deposited debris is compressed and absorbs most of the dynamic impact forces from the approaching debris. Given that the barrier is protected by deposits, the approaching debris is unable to reach the barrier and only a static load is induced on the barrier. The baffle arrays should be designed to focus on intercepting the granular jets, since these induce the highest dynamic impact force on the rigid barrier.

Figure 8 shows a comparison of the normalised computed dynamic force ( $F$ ) resulting from a control experiment, a single row and additional staggered rows with different row spacing ( $L$ ) normalised by the slit opening

( $D$ ). The time ( $t$ ) is taken as  $t = 0$  second when the debris front impacts the first row of baffles. The  $F$  is the difference between the total force acting on the barrier and the static load induced by debris deposits behind the barrier. The dynamic force acting on the barrier is calculated as the sum of non-static forces normal to the barrier surface. A discrete element is considered to be static with velocity less than 0.1 m/s. The  $F$  is normalised by the peak computed dynamic force ( $F_c$ ) of the control test. The control test is carried out without baffles protecting the rigid barrier.

The results revealed that the magnitude of the peak force acting on the rigid barrier with a single row array protecting the barrier is reduced by 33%, while two rows of baffles reduce the peak impact force by more than 50%. A single row allows discharge between the slits to pass through unimpeded (Figure 9(a)), whereas a second staggered row intercepts and decelerates discharge from the first row (Figure 9(b)). Successive rows of baffles positioned closer exhibit a higher reduction of impact force due to a more concentrated granular jet impacting the second staggered row (Figure 10(a)).

The presences of baffles do not result in a significant reduction of impact force during the run-up stage. As shown in Figure 8, the normalised impact force of the control case (without baffles) during the run-up stage is not the highest among all the impact cases. The higher impact force with baffles during the run-up stage is explained by the phenomenon of debris overflowing the baffles and impacting on the rigid barrier. The relatively high impact force caused by overflowing debris is promoted by closely-spaced rows of baffles which facilitates the formation of a ramp-like deposition behind the second row (Figure 10(b)).

During the pile-up stage, the granular deposits protect the barrier from dynamic impact. Hence, there is no obvious effect of the baffle arrays on the barrier during the pile-up stage and the impact forces are similar to the control case for all baffle arrangements.

### Optimum configuration

Key findings for spacing between successive rows, baffle height, number of rows and transverse blockage ( $T_b$ ) of baffle arrays are discussed in the following sections.

#### Spacing between successive rows

As previously discussed, granular jet impact forces are reduced by adopting narrower  $L$ , while impact from overflowing debris is reduced with wider  $L$ . Given this dilemma, there should be an optimum distance for  $L$  which reaches a compromise between suppressing granular jet impact and overflow forces. Figure 11 shows the relationship between the baffle spacing ( $L/D$ ) and

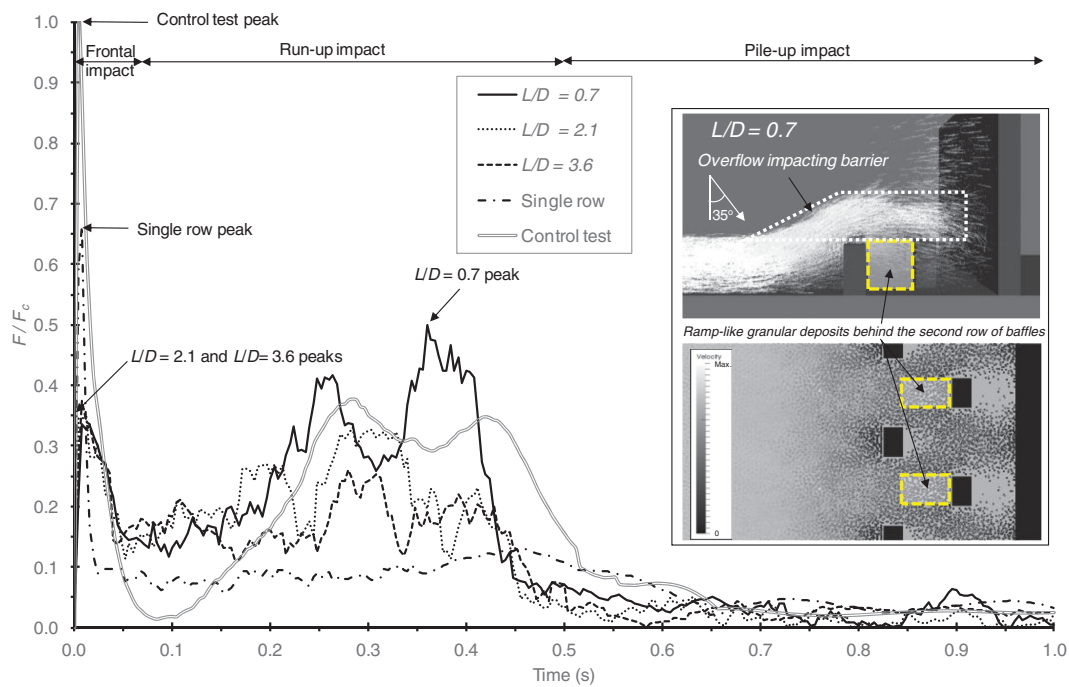


Figure 8. Computed normalised dynamic force with different row spacing ( $L$ ).[12]

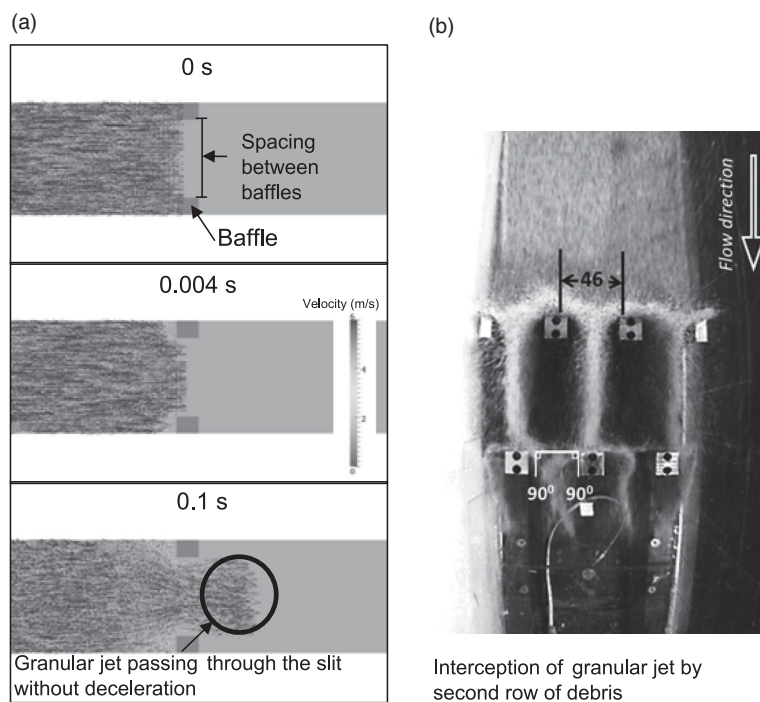


Figure 9. Influence of  $D$  between baffles: (a) non-decelerating frontal debris passing through slit [13]; (b) interception of frontal debris by second row (all dimensions in mm).[5]

the computed normalised peak dynamic force. The normalised peak dynamic force for arrays with different  $L$  is obtained from data extracted from Figure 8. The optimum spacing, or the lowest dynamic force, is observed at a configuration of about  $L/D = 3$ . A drop of  $L/D$  below 3 results in the higher peak impact forces caused by

overflowing. It is apparent that a reduction of around 35% of the peak impact force is achieved by increasing  $L/D$  from 0.7 to 3. Adopting a value of  $L/D$  greater than 3 leads to a reduced effect of the second row. An increase of around 25% of peak impact force is exhibited by increasing  $L/D$  from 3 to 4.3.

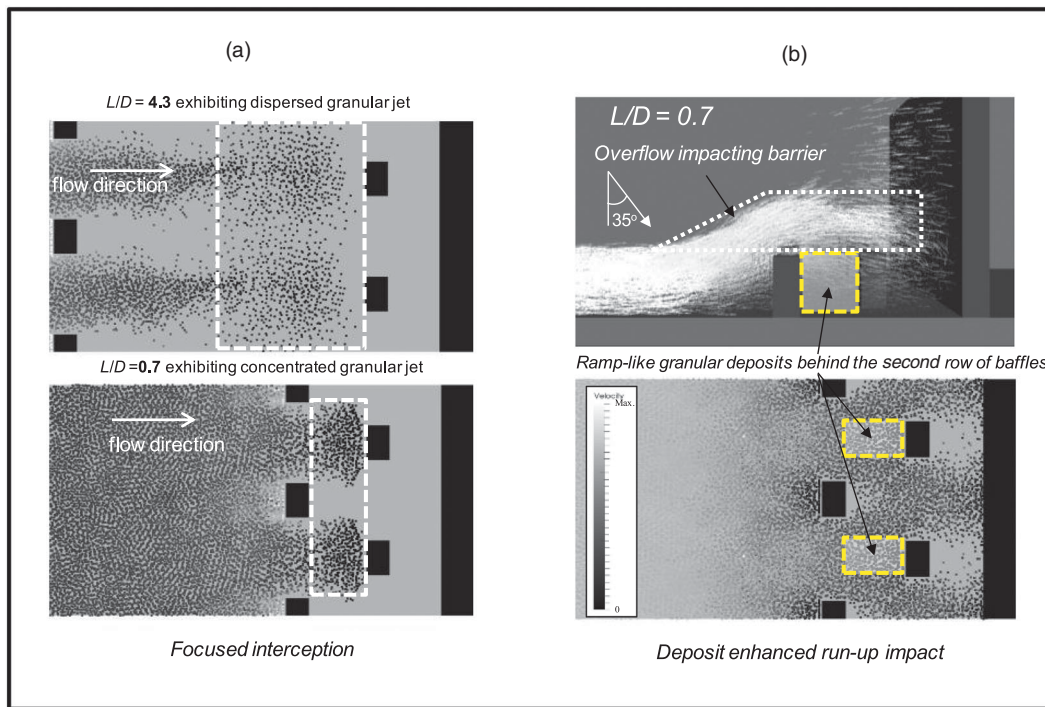


Figure 10. Influence of spacing between successive rows: (a) comparison of narrow and wide  $L$ ; (b) overflow resulting from ramp-like dead zone formation.

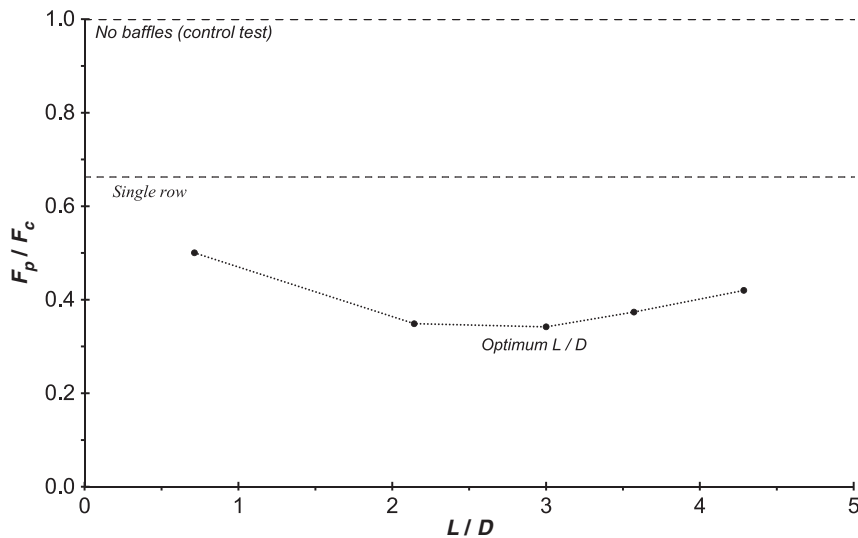


Figure 11. Effect of baffle spacing ( $L/D$ ) on the computed peak dynamic force.[12]

**Baffle height**

While it is reasonable to assume that a greater baffle height always results in better protection to the downstream terminal barrier, the cost effectiveness of extending the baffle height needs to be studied. Figure 12 shows a comparison of the normalised impact force from two row baffle arrays with heights ranging from  $0.75 h$  to  $2.5 h$ . The optimum row spacing,  $L/D = 3$ , was selected

for comparison. The peak impact force is noticeably reduced when the baffle height is increased from  $0.75 h$  to  $1.5 h$ . As discussed previously, the peak impact force for  $L/D > 0.7$  is contributed solely by the granular jets (Figure 11). A baffle height of  $0.75 h$  is ineffective in decelerating the granular jets, since the formation of a ramp-like deposition leads to overflow impacting the rigid barrier. Further increasing the baffle height beyond

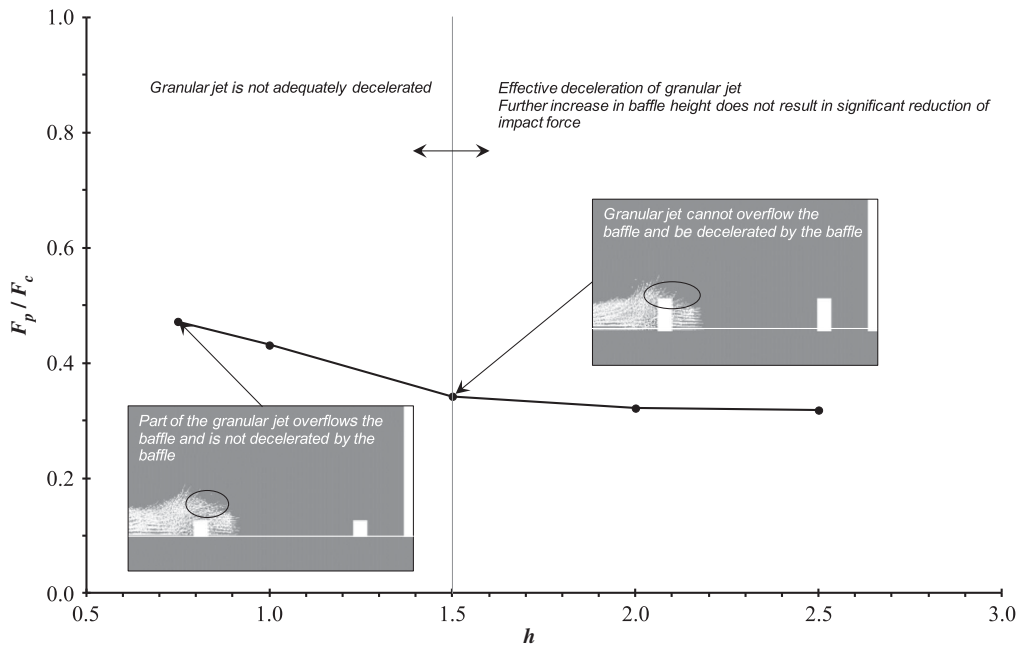


Figure 12. Effect of baffle height on the peak dynamic force.[12]

1.5  $h$  does not result in any significant decrease in the peak impact force, hence a baffle height of 1.5  $h$  is considered optimal.

**Number of rows**

The function of baffles is to perturb the flow pattern such that flow slows down as it approaches each block and then accelerates as it passes each block towards the next row.[7] At least two rows in staggered formation are required to intercept granular jets discharging from the slits of the first row of baffles. The impact of granular jets against a second staggered row and the further division of these jets is one of the contributing interaction mechanisms for energy loss resulting from increasing the number of rows (Figure 7(c)).

**Transverse blockage**

To ensure that landslide debris baffles are installed instead of slit dams, two empirical criteria for slit dams are adopted. The  $D$  normalised by the maximum particle size ( $d_{max}$ ) should fall outside the range of the following relationship proposed by Watanabe et al. [27] for slit dams:

$$D/d_{max} < 2.0. \tag{2}$$

Furthermore, the ratio of the summation of  $D$  across the width of the channel over the channel width ( $w$ )

should fall outside the range of the following relationship proposed by Ikeya and Uehara [28] for slit dams:

$$\sum D/w = 0.2 \sim 0.6. \tag{3}$$

A one-dimensional representation of obstruction (independent of the baffle height) along the transverse direction can be characterised using the degree of  $T_b$ :

$$T_b = \sum D/w \times 100. \tag{4}$$

For the array to act as baffles instead of a slit dam, it must be less than an equivalent of 40% of the  $T_b$ .

A study of landslide debris mobility using flume experiments [5] shows that adopting the maximum  $T_b$  of 40% may not be the most effective solution, since a higher degree of obstruction promotes overflow. Figure 13 shows a comparison of the mobility resulting from baffle arrays with degrees of  $T_b$  ranging from 0% to 37%. The optimum baffle height is adopted (1.5  $h$ ). The runout distance of each experiment is characterised with the travel angle. The travel distance is commonly assessed using the travel angle,[29,30] since strong empirical correlations between the apparent friction and travel angle are ideal for numerical analysis.[3] Figure 11 shows correlations between travel angles and baffles of varying configurations. A schematic is imposed on Figure 13 to define the travel angle. The results reveal that increasing the degree of  $T_b$  from 20% to 30% leads to reduced mobility (higher travel angles). However, increasing the

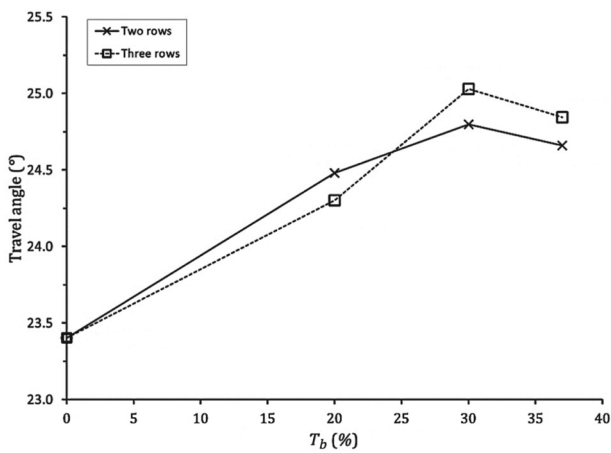


Figure 13. Comparison of travel for different degree of  $T_b$ .

$T_b$  from 30% to 37% results in increased mobility (lower travel angles). Moreover, this phenomenon is attributed to pronounced overflow processes with higher cross-sectional blockage within the channel. Based on mobility tests, it was assessed that  $T_b = 30%$  is the optimum configuration.

**Energy dissipation characteristics**

To understand the energy dissipation characteristics, the normalised kinetic energy of discrete elements discharging through a single row of baffles was investigated (Figure 14). Computed results were obtained from

Choi et al. [11]. The single row of baffles has a  $T_b$  of 30% and each baffle has a height of 120 mm or 1.5 times the initial approaching flow depth before impact. The normalised kinetic energy is the average computed kinetic energy of discrete elements ( $E_k$ ) divided by the kinetic energy of the initial approaching debris front before impact ( $E_a$ ). Monitoring sections were imposed downstream of the array of baffles with increments of 30 mm from the downstream face of the baffles, as illustrated in the schematic. The downstream monitoring sections with increasing distance away from the array of baffles are denoted as D1 to D6. Two reference lines are provided to estimate the normalised energy dissipation predicted from an empirical criteria (Salm [31]) and as measured in flume experiments for much higher supercritical flows,  $Fr$  of about 10 to 12.

As the debris front discharges from the row of baffles, an increase in normalised kinetic energy occurs, which is attributed to the flow front discharging through a reduced flow area. The kinetic energy of the flow rapidly decreases to about 0.5 times the value of the initial upstream condition, before a slight increase in kinetic energy from overflow is observed. With an increasing downstream distance from D1 to D6, it is evident that similar energy dissipative behaviour is exhibited; however, the kinetic energy diminishes with distance. Given that Johannesson et al. [8] carried out experiments with much higher supercritical flows, the estimated energy loss is higher than that observed in Choi et al. [11]. Furthermore, the empirical relationship proposed by Salm [31] only accounts for the upstream area within the channel in

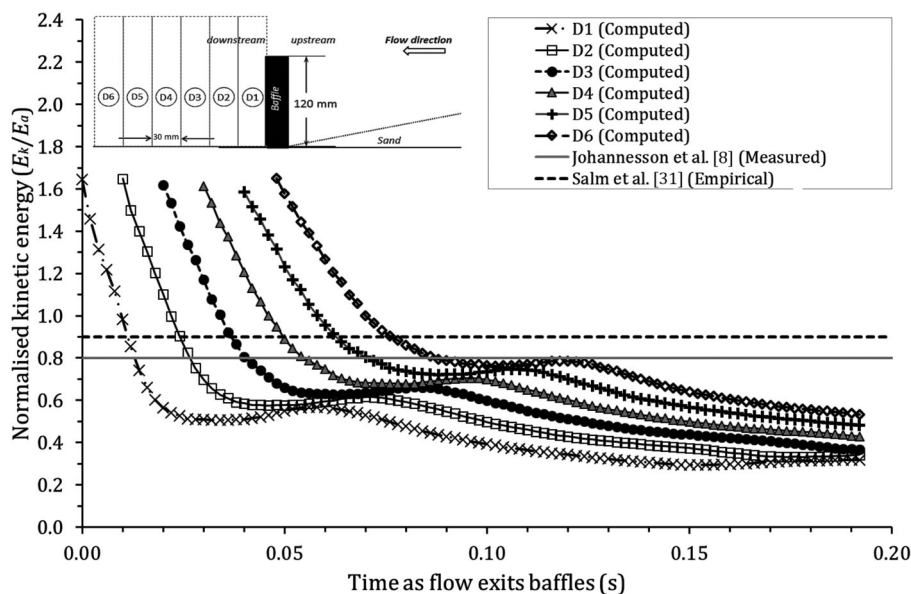


Figure 14. Typical downstream kinetic energy dissipation characteristics for a single row of 1.5  $h$  baffles with 30%  $T_b$ . [11]

Table 2. Summary of the optimum configurations for an array of baffles.

Geometric parameter	Optimum configuration	Remarks
Spacing between successive rows ( $L$ )	$L/D = 3$	Effective reduction of both granular jet and overflow impact.
Baffle height	$1.5 h$	Further increase in height does not result in significant reduction of impact force.
$T_b$	30%	$T_b$ exceeding 30% have demonstrated excessive overflow for mobility tests.[5]
Number of rows	$\geq 2$	Given that the aforementioned geometrical configurations are met and overflow is suppressed; increasing the number of rows will increase the effectiveness of the baffle array; the rows should be in a staggered formation.

estimating the energy loss and does not account for the initial approaching flow conditions nor the flow mechanisms of the dead zone formation or overflow.

### Discussion

Landslide debris has poor temporal predictability and it is not entirely feasible to carry out full-scale tests in Hong Kong. Given these constraints, small-scale flume modelling was adopted. Physical flume test results were then used to calibrate a DEM model for numerical back analysis. The authors acknowledge that there are limitations with both small-scale modelling and the DEM, however, it is undeniable that the physics from the flume tests are real and that the calibrated DEM model can further be developed to study the problem of baffle-debris interaction.

It is also acknowledged that landslide debris consists of both poorly sorted saturated particles, and that only uniform dry granular material was investigated in this study. It is stressed that without first understanding the dynamics of dry granular material, one of the simplest flow cases, there is little hope of understanding the complex behaviour of a two-phased flow or advancing the current understanding of landslide debris-resisting baffles. Furthermore, there are a multitude of geometric configurations that can be studied, and here the focus was only on the baffle height, number of rows, spacing between successive rows and degree of  $T_b$ .

### Conclusions

Practitioners in Hong Kong currently install landslide debris-resisting baffles using prescriptive and empirical approaches without an understanding of their impact mechanisms. The performance of landslide debris-resisting baffles has not been established in literature and currently there are no design recommendations. A comprehensive study using physical modelling and numerical back analysis was carried out to provide insight into the impact mechanisms, performance and optimum configuration pertaining to landslide debris-resisting baffles.

It is evident from the results that baffles provide a substantial reduction of the peak dynamic impact force induced on rigid barriers. A summary of the optimum configuration is given in Table 2. The interaction mechanism of most concern, as observed in this study, is overflow climbing on top of a ramp-like deposition zone. Overflow generates a secondary dynamic impact force on the rigid barrier and if the appropriate geometric configuration is adopted, the adverse effects of overflow can be controlled.

### Acknowledgements

This paper is published with the permission of the Head of the Geotechnical Engineering Office (GEO) and the Director of Civil Engineering and Development, the HKSAR Government, People's Republic of China. The authors would like to gratefully acknowledge the support of the GEO of the Civil Engineering and Development Department (CEDD) of the HKSAR Government for commissioning an investigation pertaining to landslide debris-resisting baffles. The authors would also like to thank Ir Prof Charles W W Ng and the HKUST Jockey Club Institute for Advanced Study for their support. Finally, the authors would like to express their thanks to Ir Herman Y K Shiu and Ir Dr S W Lee for their comments.

### Funding

This work was supported by a grant from the Research Grants Council of the HKSAR, People's Republic of China (T22-603/15N).

### Notes on contributors



**Prof Clarence E Choi** is a faculty member in the Department of Civil and Environmental Engineering at The Hong Kong University of Science and Technology and previously practised geotechnical engineering with Golder Associates (HK) Limited. His research focuses on understanding and mitigating landslides and natural terrain hazards. He is currently a Fellow (Junior) of the HKUST Jockey Club Institute for Advanced Study.



**Ir Raymond P H Law** is a Geotechnical Engineer working in the GEO of the CEDD. He completed his Ph.D. degree at the Hong Kong University of Science and Technology and has over 10 years of experience of focused research in debris flow mechanics and the interactions of debris with structures, using numerical tools such as the

discrete element method as well as flume model tests. He also has good experience in the design of natural terrain mitigation measures in Hong Kong.

## References

- [1] AECOM. Detailed study of the 7 June 2008 landslides on the hillside above Yu Tung Road, Tung Chung. Hong Kong: Geotechnical Engineering Office, Civil Engineering and Development Department, the HKSAR Government; 2012. p. 124 (GEO report no. 271).
- [2] Volkwein A, Wendeler C, Guasti G. Design of flexible debris flow barriers. *Italian Journal of Engineering Geology and Environment*. Casa Editrice Universita La Sapienza; 2011.
- [3] Lo DOK. Review of natural terrain landslide debris-resisting barrier design. Hong Kong: Geotechnical Engineering Office, Civil Engineering and Development Department, the HKSAR Government; 2000. (GEO report no. 104).
- [4] Choi CE, Au-Yeung S, Ng CWW. Flume investigation of landslide granular debris and water runoff mechanisms. *Geotech Lett*. 2015;5(1):28–32.
- [5] Ng CWW, Choi CE, Song D, et al. Physical modelling of baffles influence on landslide debris mobility. *Landslides*. 2014;12(1):1–18.
- [6] United States Bureau of Reclamation. Design of small dams. 3rd ed. Washington (DC): United States Department of the Interior; 1987.
- [7] United States Federal Highway Administration. Hydraulic design of energy dissipators for culverts and channels. Hydraulic engineering circular no. 14. National Highway Institute, 3rd ed. Springfield (VA): National Highway Institute; 2006.
- [8] Jóhannesson T, Gauer P, Issler D, Lied K. The design of avalanche protection dams recent practical and theoretical developments. Belgium: European Commission; 2009.
- [9] Choi CE. Flume and discrete element investigation of granular flow mechanisms and interaction with baffles [Ph.D. thesis]. Hong Kong: Department of Civil and Environmental Engineering, The Hong Kong University of Science and Technology; 2013.
- [10] Choi CE, Ng CWW, Song D, et al. Flume investigation of landslide debris baffles. *Can Geotech J*. 2014;51(5):540–553.
- [11] Choi CE, Ng CWW, Song D, Law RPH, Kwan JHS, Ho KKS. A computational investigation of baffle configuration on the impedance of channelized debris flow. *Can Geotech J*. 2014;52(2):182–197.
- [12] Law RPH, Choi CE, Ng CWW. Discrete element investigation of the influence of debris flow baffles on rigid barrier impact. *Can Geotech J*. 2015. doi:10.1139/cgj-2014-0394.
- [13] Law RPH. Computational study of granular debris flow impact on rigid barriers and baffles [Ph.D. thesis]. Hong Kong: Department of Civil and Environmental Engineering, The Hong Kong University of Science and Technology; 2015.
- [14] Hubl J, Suda J, Proske D, Kaitna R, Scheidl C. Debris flow impact estimation. Proceedings of the 11th International Symposium on Water Management and Hydraulic Engineering; 2009 Sep 1–5; Ohrid, Macedonia; p. 137–148.
- [15] Armanini A, Larcher M, Odorizzi M. Dynamic impact of debris flow against a vertical wall. *Ital J Eng Geol Environ*. 2011;11:1041–1049.
- [16] Ng CWW, Choi CE, Kwan JHS, Shiu HYK, Ho KKS, Koo RCH. Flume modelling of debris flow resisting baffles. Proceedings of AGS Seminar on Natural Terrain Hazards Mitigation Measures, AGS, the HKSAR Government; 2012 Oct 16. p. 16–21.
- [17] Kloss C, Goniva C. Liggghts—a new open source discrete element simulation software. Proceedings of the 5th International Conference on Discrete Element Methods; 2010 Aug 25–26. p. 25–26.
- [18] Rapaport DC. The art of molecular dynamics simulation. 2nd ed. Cambridge University Press; 2004. ISBN 0-521-82568-7.
- [19] Teufelsbauer H, Wang Y, Pudasaini SP, Borja RI, Wu W. DEM simulation of impact force exerted by granular flow on rigid structures. *Acta Geotech*. 2011;6(3): 119–133.
- [20] Chiou MC. Modelling dry granular avalanches past different obstructions: numerical simulations and laboratory analyses [dissertation]. Germany: Technical University Darmstadt; 2005.
- [21] Pudasaini SP, Hsiau S, Wang Y, Hutter K. Velocity measurements in dry granular avalanches using particle image velocimetry-technique and comparison with theoretical predictions. *Phys Fluids*. 2005;17(9):1–10.
- [22] Pudasaini SP, Hutter K. Avalanche dynamics: dynamics of rapid flows of dense granular avalanches. Berlin: Springer; 2007.
- [23] Chau KT, Wong RHC, Wu JJ. Coefficient of restitution and rotational motions of rockfall impacts. *Int J Rock Mech Min Sci*. 2002;39:69–77.
- [24] Azzoni A, Freitas MH. Experimentally gained parameters, decisive for rock fall analysis. *Rock Mech Rock Eng*. 1995;28(2):111–124.
- [25] Robotham ME, Wang H, Walton G. Assessment of risk from rockfall from active and abandoned quarry slopes. *Trans Inst Min Metall*. 1995;104:25–33.
- [26] Gray JMNT, Tai YC, Noelle S. Shock waves, dead zones and particle-free regions in rapid granular free-surface flows. *J Fluid Mech*. 2003;491:161–181.
- [27] Watanabe M, Mizuyama T, Uehara S. Review of debris flow countermeasure facilities. *J Jpn Erosion Control Eng Soc*. 1980;115:40–45. Japanese.
- [28] Ikeya H, Uehara S. Experimental study about the sediment control of slit Sabo dams. *J Jpn Erosion Control Eng Soc*. 1980;114:37–44. Japanese.
- [29] Heim A. *Bergsturz und Menschenleben*. Zurich: Fretz and Wasmuth Verlag; 1932. p. 218.
- [30] Scheidegger A. On the prediction of the reach and velocity of catastrophic landslides. *Rock Mech*. 1973;5: 231–236.
- [31] Salm B. 1987. Snow, avalanches and avalanche protection (lecture notes). Swiss Federal Institute of Technology in Zurich. [In German.]